

Received: 04 February 2022 • Accepted: 24 March 2022

## Research

doi: 10.22034/jcema.2022.328603.1080

# Simulated C<sub>3</sub>A Effects on the Chloride Binding in Portland Cement with NaCl and CaCl<sub>2</sub> Cations

Jafar Sobhani <sup>1\*</sup>, Fatemeh Jafarpour <sup>2</sup>, Fahimeh Firozyar <sup>2</sup>, Ali Reza Pourkhorshidi <sup>2</sup><sup>1</sup>Associate professor, Road, Housing and Urban Development Research Center, Tehran, Iran.<sup>2</sup>Road, Housing and Urban Development Research Center, Tehran, Iran.

\*Correspondence should be addressed to Jafar Sobhani, Department of Civil Engineering, Road, Housing and Urban Development Research Center, Tehran, Iran. Tel: +982188255942; Fax: +982188255942; Email: [ja\\_sobhani@yahoo.com](mailto:ja_sobhani@yahoo.com), [sobhani@bhrc.ac.ir](mailto:sobhani@bhrc.ac.ir).

## ABSTRACT

C<sub>3</sub>A contents of Portland cement have a significant role in chloride ion binding in chloride-contaminated environments. Cations released due to NaCl and CaCl<sub>2</sub> in chloride environments are the most common and aggressive agents. In this research, various simulated pure C<sub>3</sub>A were made using calcium hydroxide and aluminum hydroxide, including 5%, 8%, 10%, and 12%. Moreover, the different concentrations of sodium and calcium cations in NaCl and CaCl<sub>2</sub> in the simulated Portland cement paste were added the bonding performances were investigated. X-ray diffraction (XRD) of prepared C<sub>3</sub>A samples identified for major phases of specimens. Thermo-gravimetry analysis (TGA) was used to quantify the simulated C<sub>3</sub>A. Standard test methods, including ASTM C1152 and ASTM C1218, were utilized to measure the acid-soluble and water-soluble chloride in prepared specimens, respectively. The results showed that the amount of acid-soluble and water-soluble chloride for NaCl and CaCl<sub>2</sub> cations decreased with an increase of the C<sub>3</sub>A, which indicates a better chloride ion binding potential. Moreover, it was concluded that CaCl<sub>2</sub> cations have more chloride binding capacity than NaCl. For calcium cations in CaCl<sub>2</sub>, the increase of C<sub>3</sub>A is distinguished in water-soluble chloride in comparison with NaCl cations. Then, in areas contaminated with NaCl ions, it is recommendable to use more C<sub>3</sub>A content in the Portland cement.

**Keywords:** C<sub>3</sub>A content, CaCl<sub>2</sub> and NaCl cations, Portland cement, Chloride binding.

Copyright © 2022 Jafar Sobhani. This is an open access paper distributed under the [Creative Commons Attribution License](#). *Journal of Civil Engineering and Materials Application* is published by [Pendar Pub](#); Journal p-ISSN 2676-332X; Journal e-ISSN 2588-2880.

## 1. INTRODUCTION

Chloride-induced steel corrosion is one of the major worldwide deterioration mechanisms for reinforced concrete structures. Concentrations of chloride ions in sufficient amounts are considered essential parameters for inert ferric oxide film around the steel reinforcement, which typically inhibits the steel from corrosion in the alkaline environment of dense concrete [1-2]. Specifications usually express corrosion hazards in terms of total chloride in concrete as a percentage of cement content. However, a significant portion of the total chloride is chemically synthesized or adsorbed by solid cement hydrates [3]. Such chlorides attached to solid hydration products of cement are non-corrosive and do not

pose a risk of corrosion. It is the concentration of the indirect chloride fraction that dissolves in the liquid phase of the concrete and causes it to decompose due to its ability to destroy the protective film and the corrosion process of the steel. Due to this situation, the distribution of chloride ions between the solution phase of aqueous pores and solid hydration products of cement pastes is of great importance from the point of view of starting and spreading the risk of corrosion for reinforcements embedded in chloride concrete [4-5]. The existence of water-soluble chloride in cement mixtures, such as concrete and mortar, can cause corrosion of reinforcements. The chloride ion comes into a chemical reaction with the C<sub>3</sub>A phase and produces

chloroaluminate [6]. The chloride ions ingress or are involved in concrete in two major types: (i) internal chlorides (i.e. chlorides present at the time of mixing); and (ii) external chlorides (i.e. chlorides derived from an external source such as seawater or deicing salts). In addition, the chloride cations that come from NaCl, CaCl<sub>2</sub>, KCl, and salts have a significant effect on the amount and intensity of reinforcing steel corrosion [7-8]. According to the conducted studies, the type of chloride cations is effective in reinforcement corrosion. CaCl<sub>2</sub>, NaCl is the most common aggressive salts exposed to concrete structures. The results of the researches showed that corrosion intensity is remarkably subject to cation types [7-9]. Also, it has been shown that the total porosity and chloride concentration in pores solution or pH are not factors controlling corrosion intensity, because they were the same in all samples of the study. The difference is in electrical resistivity of a factor of difference against corrosion intensity. Whereas electrical resistivity is subject to the size distribution of mortar pores, change in cations brings about change in the size distribution of pores. Meanwhile, according to the results of the studies conducted in this regard, NaCl decreases pores sizes, and concrete porosity is, therefore, subject to concrete mixture type and cations [10-11]. In 2018, Cheng et al. studied the bonding capacity of a type of coal gangue at the initial phase of hydration, and they found that the ability to bind increased and then decreased with increasing molar ratios

of Ca/Si and Si/Al [12]. In 2020, Chunyu Qiao investigated the binding capacity of Portland cement paste containing fly ash exposed to CaCl<sub>2</sub> solution. They found that the addition of fly ash contributed to the chloride binding capacity of the cement paste. The binding capacity increased at the beginning of the paste hydration and then decreased with the formation of the CSH phase, which is due to the change in the pH of the cement paste environment [13]. In 2013, Xu et al. investigated the binding of chloride added to blended cement in sulfate exposure conditions. The results showed that after the sulfate attack, Friedel's salt was converted to Ettringite, which helps release bonded chlorides. In their studies, they introduced the Cl-/OH- index in the effect of cement-containing blast furnace slag on chloride binding capacity [14]. In addition, the amount of bonded chloride in cement containing limestone, metakaolin, and other mineral admixtures has been investigated [15-17]. In 2010, Cheewaket et al. also investigated the effects of long-term performance of fly-ash contained concretes on chloride binding capacity in marine environments [18]. Zunino and Scrivener studied the influencing factors related to the sulfate balance in pure phase C<sub>3</sub>S/C<sub>3</sub>A systems via various C<sub>3</sub>A contents added to the simulated Portland cement paste. Then different concentrations of NaCl and CaCl<sub>2</sub> cations were measured, and then the influence of these cations on the binding capacity was assessed [19].

## 2. MATERIALS AND METHODS

### 2.1. C<sub>3</sub>A PREPARATION

#### 2.1.1. Liquefaction Assessment Based on Energy Method

Based on the Phase diagram of the CaO-Al<sub>2</sub>O<sub>3</sub> system depicted in Figure 1, pure C<sub>3</sub>A is made using calcium hydroxide and aluminum hydroxide. Figure 2 shows the

laboratory furnace with a maximum temperature of 1800 °C for C<sub>3</sub>A preparation. Table 1 summarizes the C<sub>3</sub>A sample's stoichiometric ratios and their properties.

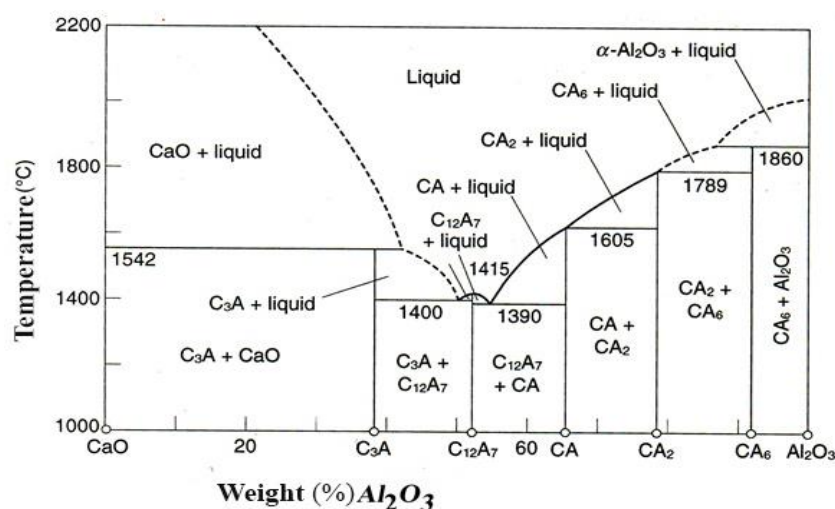


Figure 1. Equilibrium phase diagram for the CaO-Al<sub>2</sub>O<sub>3</sub> system



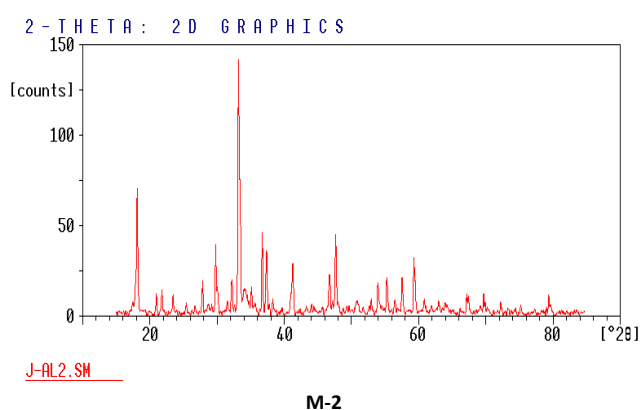
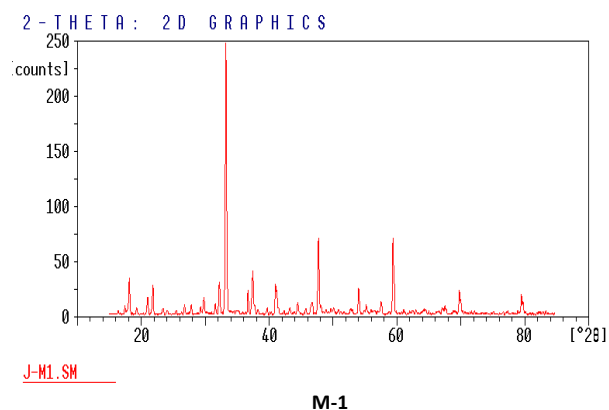
**Figure 2.** Laboratory furnace with a maximum temperature of 1800 °C for  $C_3A$  preparation

**Table 1.** Properties of  $C_3A$  samples

Sample code	Chemical composition	Stoichiometric ratios		Oven temperature (°C)	Time to reach oven temperature (min)	Oven time (min)
		$Al_2O_3$	CaO			
M-1	$Al(OH)_3 + Ca(OH)_2$	3.73	6.27	1350	330	180
M-2	$Al(OH)_3 + Ca(OH)_2$	3.73	6.27	1350	330	180
M-3	$Al(OH)_3 + Ca(OH)_2$	3.78	6.22	1350	75	15
Al-4	$Al(OH)_3 + Ca(OH)_2$	3.78	6.22	1350	75	15
M-5	$Al(OH)_3 + Ca(OH)_2$	3.85	6.15	1350	80	5
M-6	$Al(OH)_3 + Ca(OH)_2$	3.95	6.05	1350	80	5
M-7	$Al(OH)_3 + Ca(OH)_2$	4.00	6.00	1350	80	5
M-8	$Al(OH)_3 + Ca(OH)_2$	5.80	8.30	1350	80	5
M-9	$Al(OH)_3 + Ca(OH)_2$	5.80	8.30	1350	80	5

[Figure 3](#) the XRD of prepared  $C_3A$  samples, respectively. As can be seen, XRD data identified the three major phases of specimens as Tricalcium aluminate ( $Ca_3Al_2O_6$ ), Mayenite ( $Ca_{12}Al_{14}O_{33}$ ), and Calcium oxide (CaO). [Figure 4](#) shows the thermo-gravimetry analysis (TGA) using STA-449 C. [Figure 5](#) compares TG curves of 9 samples baked in the furnace by STA method with a maximum applied temperature of 1350 °C, rate of temperature rise of 10 °C/min, and retaining at a final temperature of 2 min.

Considering the data analysis of TG and XRD revealed that the  $C_3A$  ( $Ca_3Al_2O_6$ ) melts at the temperature of 1544 °C and forms a liquid phase. In 9 samples, based on TG data, the first pick could be observed in the temperature range of 454 to 420 °C related to  $Ca(OH)_2$ , which not reacted and decomposed to CaO and  $H_2O$ . Weight loss calculated through TG temperature picks denotes thermal decompositions. The results of  $Ca(OH)_2$  weight loss are presented in [Table 2](#).



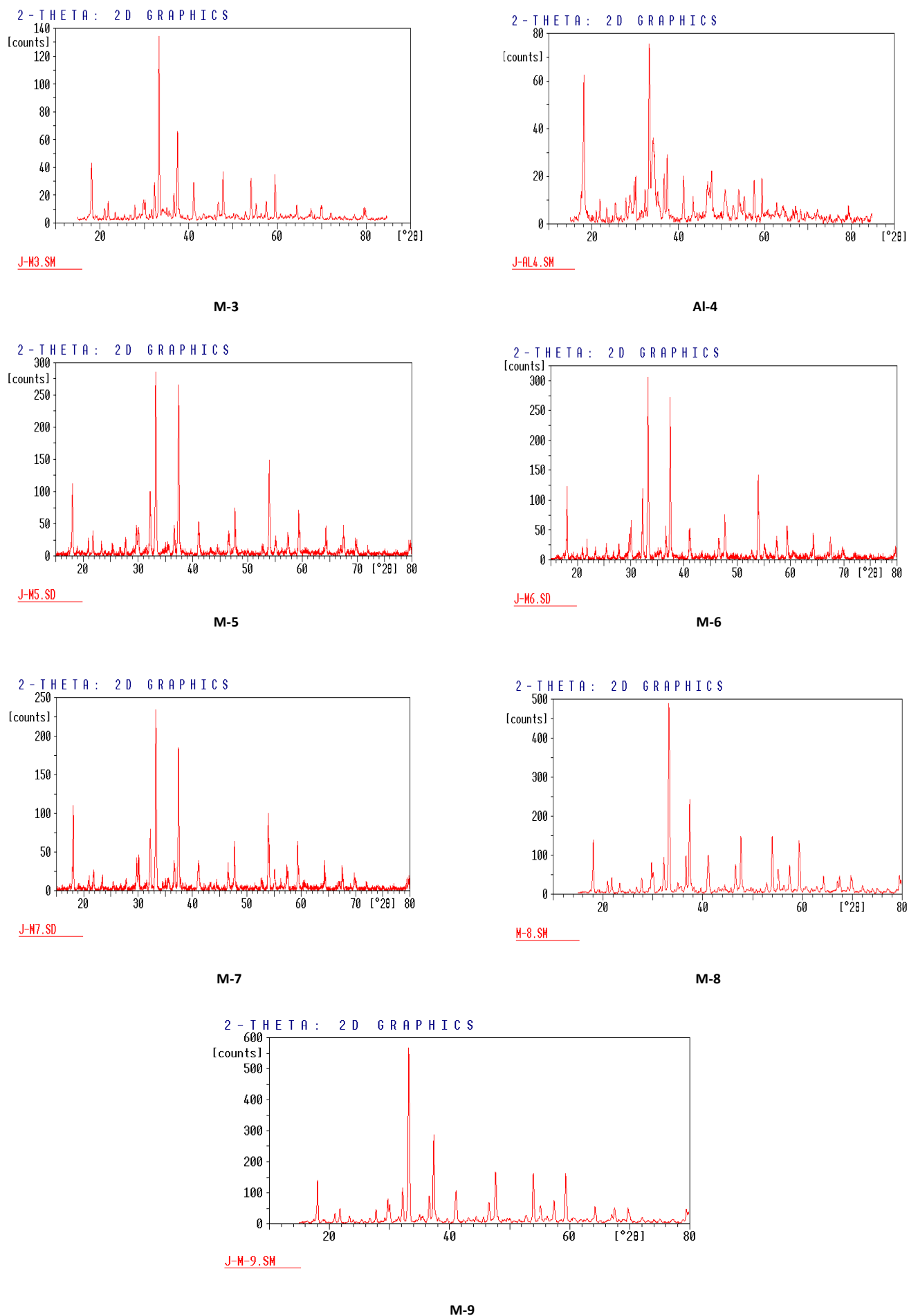
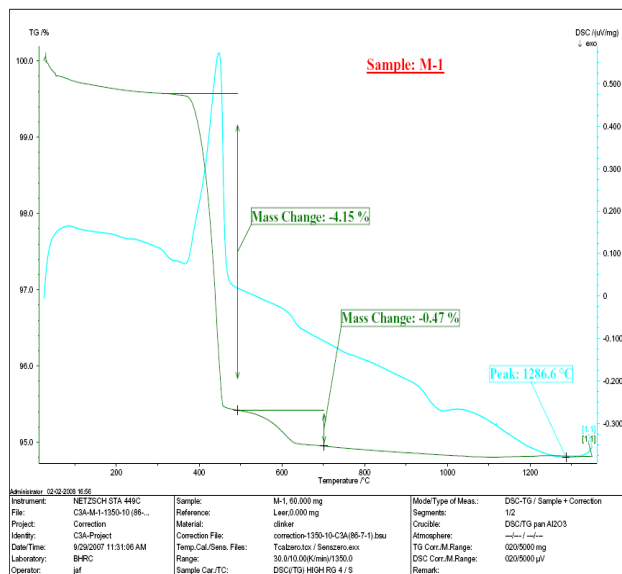
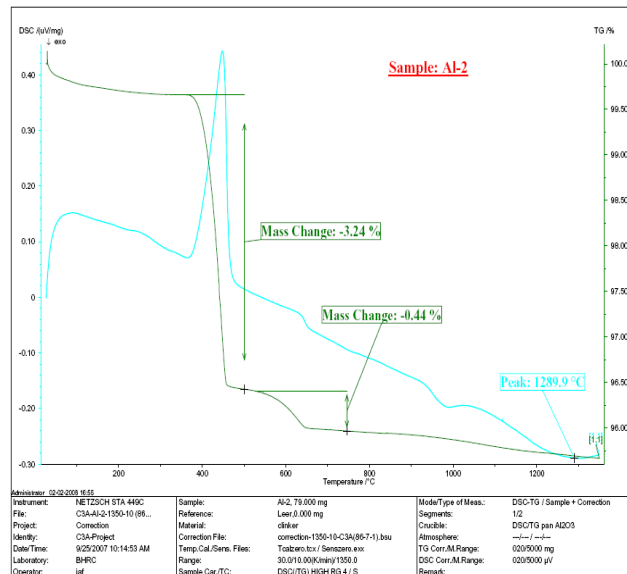


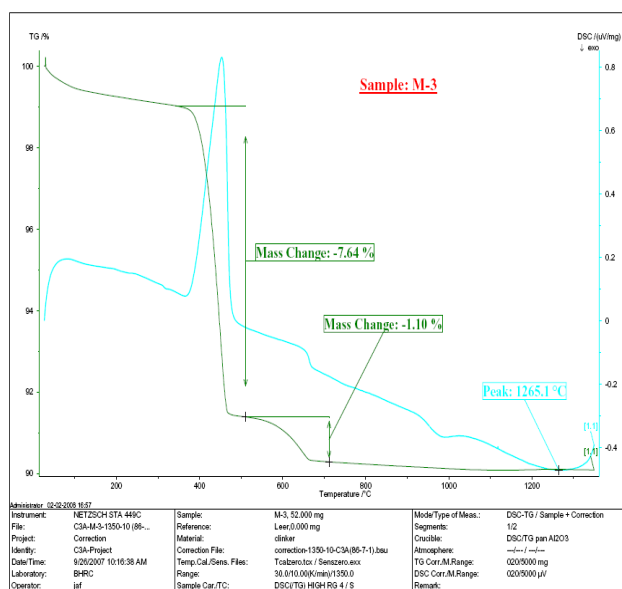
Figure 3. XRD of C<sub>3</sub>A samples



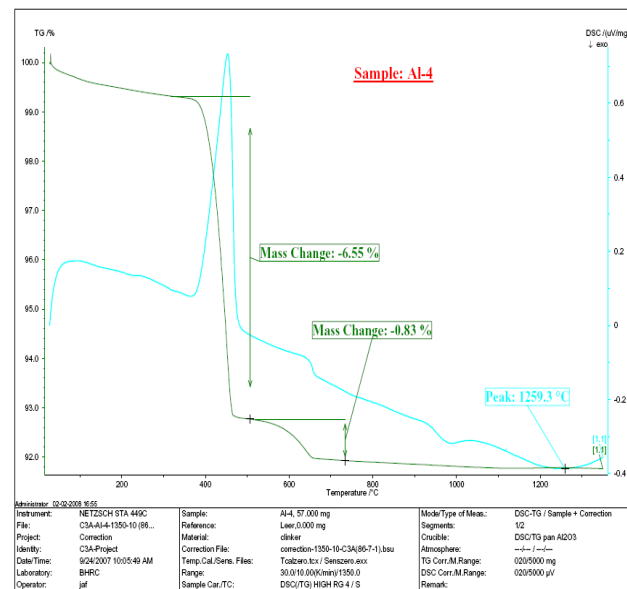
M-1



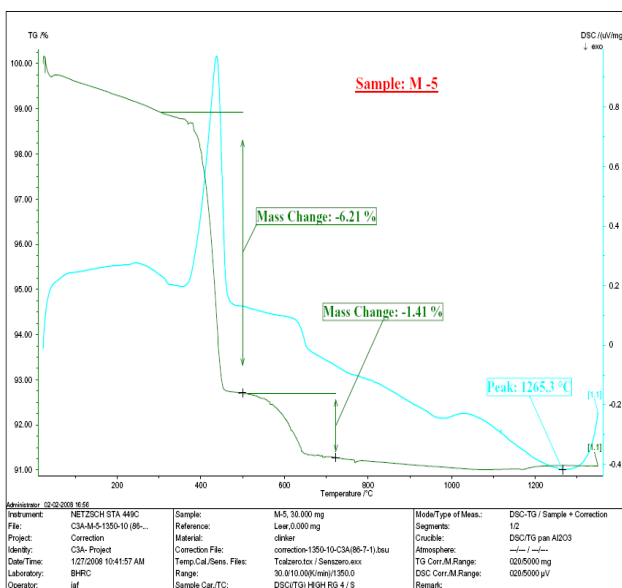
M-2



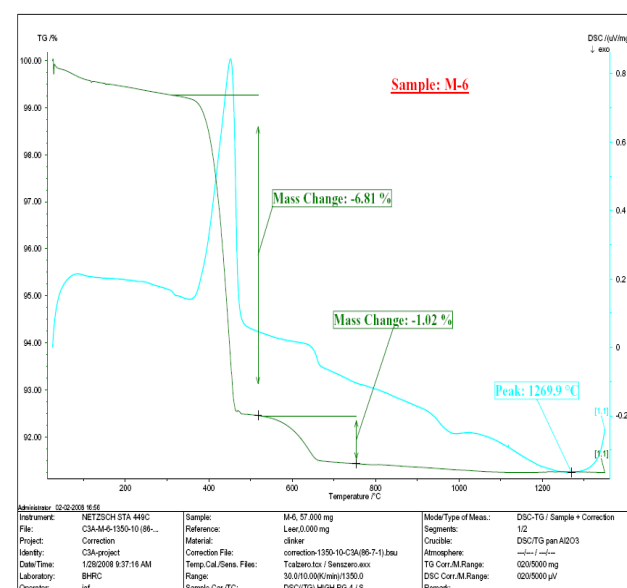
M-3



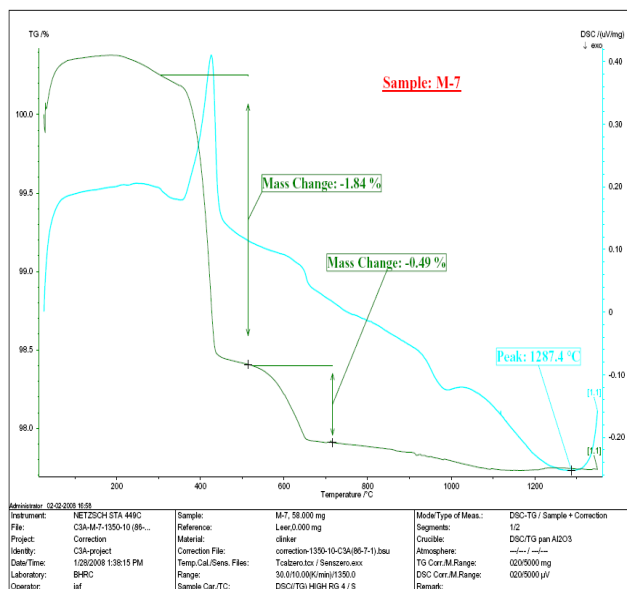
AI-4



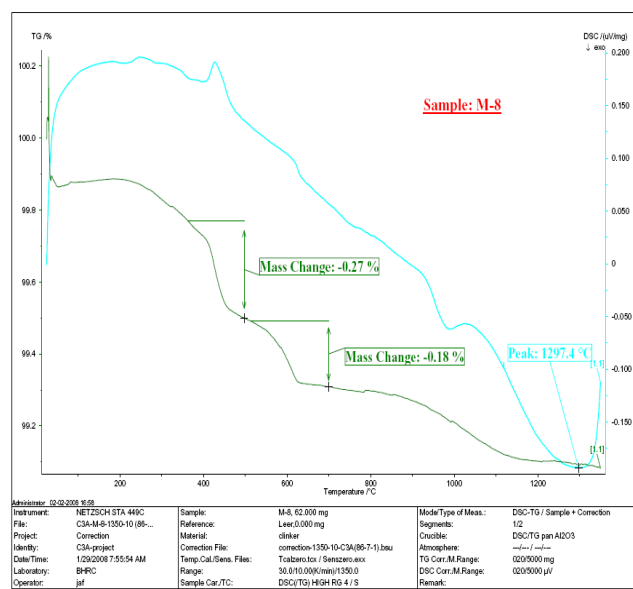
M-5



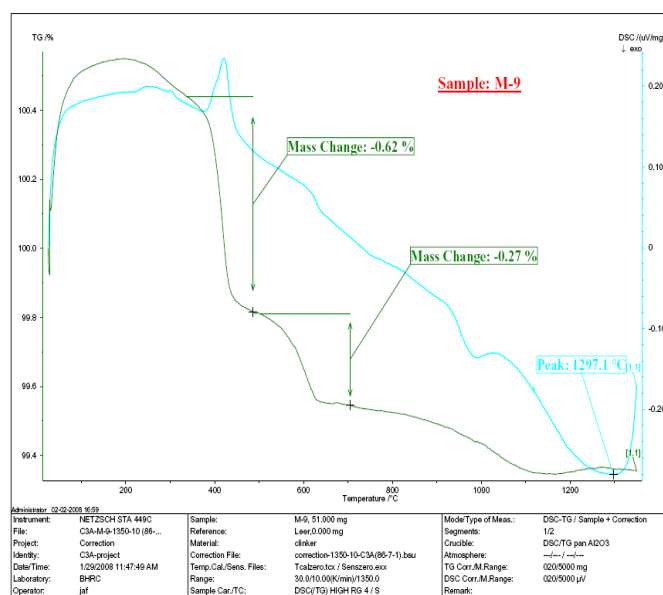
M-6



M-7



M-8



M-9

Figure 4. TG analysis of C<sub>3</sub>A samplesTable 2. C<sub>3</sub>A weight loss due to Ca(OH)<sub>2</sub> decomposition in TG analysis

Sample	Weight loss (%)	Free CaO (%)
M-1	4.15	12.91
Al-2	3.24	10.08
M-3	7.64	23.80
M-4	6.55	20.38
M-5	6.21	19.32
M-6	6.81	21.19
M-7	1.84	5.72
M-8	0.27	0.84
M-9	0.62	1.93

In Figure 5, TG curves for 9 samples were compared. As seen, for samples completely cooked, the decomposition

period time of Ca(OH)<sub>2</sub> is very short. As can be seen, the TG curve of M-8 revealed the best behavior.

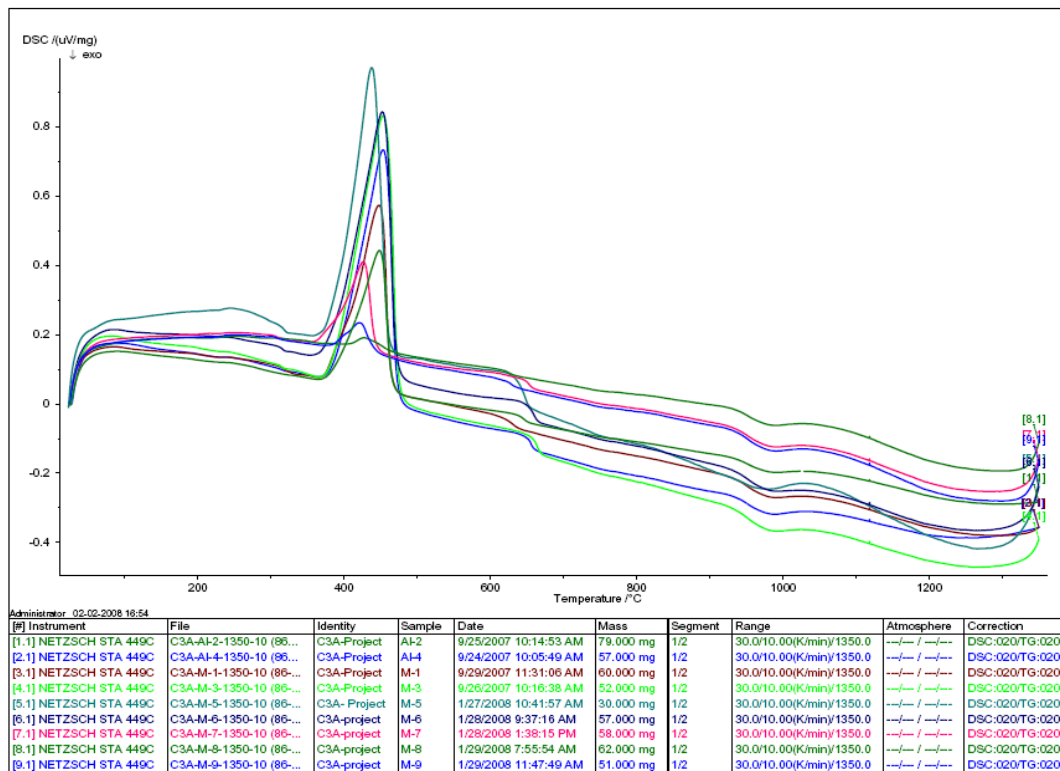


Figure 5. Comparison of TG curves of 9 samples baked in the furnace by STA method

The second temperature peak could be seen at 697 °C to 754 °C, which is related to the thermal decomposition of the  $\text{Al}(\text{OH})_3$  that did not react. The weight loss calculated through the mentioned peaks related to the TG curve, showed that the amounts of unreacted  $\text{Al}(\text{OH})_3$  are very small. The third temperature peak, which was observed at the temperature range of 973 °C to 984 °C, is related to the formation of Mayenite with the formula of  $\text{Ca}_{12}\text{Al}_2\text{O}_6$ . The fourth temperature peak, which is observed at 1259 °C to

1297 °C, is related to the formation of  $\text{C}_3\text{A}$  with the chemical formula of  $\text{Ca}_3\text{Al}_2\text{O}_6$ . The formation of Tricalcium aluminate, Mayenite and calcium oxide could be confirmed by XRD analysis, as seen in Figure 3. In summary, M-8 demonstrated a more suitable stoichiometric ratio than other samples, and the baking process was completed at 1350 °C. According to the results, M-8 was considered in this study.

## 2.2. MATERIALS

Customized factory-made Portland cement with  $\text{C}_3\text{A} < 0.5\%$  was utilized with the chemical composition of Table 3. Four laboratory-made types of cement (denoted as MC1-MC4) were produced with the addition of 5%, 8%, 10%, and 12% of pure  $\text{C}_3\text{A}$  were considered to study. Pure

sodium chloride ( $\text{NaCl}$ ) and calcium chloride ( $\text{CaCl}_2$ ), and tap water were used in sample preparation. Table 4 summarizes the details of the prepared 28 model cement samples

Table 3. Properties of utilized Portland cement

Compound/ Property	Cement
Calcium oxide ( $\text{CaO}$ )	66.20
Silica ( $\text{SiO}_2$ )	22.18
Alumina ( $\text{Al}_2\text{O}_3$ )	2.50
Iron oxide ( $\text{Fe}_2\text{O}_3$ )	4.80
Magnesium oxide ( $\text{MgO}$ )	2.4
Sodium oxide ( $\text{Na}_2\text{O}$ )	0.23
Potassium oxide ( $\text{K}_2\text{O}$ )	0.13
Sulfur trioxide ( $\text{SO}_3$ )	1.35
Loss on ignition (975°C)	0.65
Tri calcium aluminate ( $\text{C}_3\text{A}$ )	<0.5



Batches consisting of 1.5 kg of each of the cement paste mixes shown in [Table 4](#) were cast in cylindrical PVC molds (49mm dia.×100mm long) and compacted by vibration ([Figure 6](#)). The molds were sealed and the

specimens stored in a steam room for up to 24 hours, then de-molded and moist-cured for 28 days. [Figure 7](#) shows the potentiometer for chloride ion measurements.



**Figure 6.** Samples made in the laboratory



**Figure 7.** Potentiometer for chloride ion measurement

**Table 4.** Detail of specimens

Sample ID	Characteristics	W/C	NaCl (%)	CaCl <sub>2</sub> (%)
C1	MC1 (Cement+5% pure C <sub>3</sub> A)	0.32	0	0
C2			0.5	0
C3			1.0	0
C4			2.0	0
C5			0	0.5
C6			0	1.0
C7			0	2.0
C8	MC2(Cement+8% pure C <sub>3</sub> A)	0.32	0	0
C9			0.5	0
C10			1.0	0
C11			2.0	0
C12			0	0.5
C13			0	1.0
C14			0	2.0



C15	MC3 (Cement+10% pure C <sub>3</sub> A)	0.32	0	0
C16			0.5	0
C17			1.0	0
C18			2.0	0
C19			0	0.5
C20			0	1.0
C21			0	2.0
C22	MC4 (Cement+12% pure C <sub>3</sub> A)	0.32	0	0
C23			0.5	0
C24			1.0	0
C25			2.0	0
C26			0	0.5
C27			0	1.0
C28			0	2.0

### 3. RESULTS AND DISCUSSION

Standard test methods as per ASTM C1152 [20] and ASTM C1218 [21] were utilized to measure the acid-soluble and water-soluble chloride in prepared specimens,

respectively. A potentiometer with an AgNO<sub>3</sub> electrode was used for measurements of chloride content in the specimens. The results are summarized in [Tables 5-8](#).

**Table 5.** Results of chloride measurements in samples with 5% of pure C<sub>3</sub>A

Sample ID	Characteristics	Chloride ion in added NaCl (%)	Chloride ion in added CaCl <sub>2</sub> (%)	Measured chloride ion with potentiometer (%)	
				Acid soluble chloride	Water soluble chloride
C1	MC1	0	0	0	0
C2		0.303	0	0.297	0.139
C3		0.607	0	0.598	0.271
C4		1.214	0	1.095	0.591
C5		0	0.320	0.298	0.111
C6		0	0.640	0.637	0.191
C7		0	1.279	1.102	0.448

**Table 6.** Results of chloride measurements in samples with 8% of pure C<sub>3</sub>A

Sample ID	Characteristics	Chloride ion in added NaCl (%)	Chloride ion in added CaCl <sub>2</sub> (%)	Measured chloride ion with potentiometer (%)	
				Acid soluble chloride	Water soluble chloride
C8	MC2	0	0	0.001	0
C9		0.303	0	0.297	0.119
C10		0.607	0	0.598	0.656
C11		1.214	0	1.112	0.526
C12		0	0.320	0.297	0.108
C13		0	0.640	0.633	0.181
C14		0	1.279	1.178	0.399

**Table 7.** Results of chloride measurements in samples with 10% of pure C<sub>3</sub>A

Sample ID	Characteristics	Chloride ion in added NaCl (%)	Chloride ion in added CaCl <sub>2</sub> (%)	Measured chloride ion with potentiometer (%)	
				Acid soluble chloride	Water soluble chloride
C15	MC3	0	0	0	0
C16		0.303	0	0.296	0.104
C17		0.607	0	0.594	0.238
C18		1.214	0	1.193	0.471
C19		0	0.320	0.308	0.102
C20		0	0.640	0.635	0.129
C21		0	1.279	1.252	0.360

**Table 8.** Results of chloride measurements in samples with 12% of pure C<sub>3</sub>A

Sample ID	Characteristics	Chloride ion in added NaCl (%)	Chloride ion in added CaCl <sub>2</sub> (%)	Measured chloride ion with potentiometer (%)	
				Acid soluble chloride	Water soluble chloride
C22	MC4	0	0	0	0
C23		0.303	0	0.289	0.094
C24		0.607	0	0.580	0.215
C25		1.214	0	1.196	0.454
C26		0	0.320	0.316	0.043
C27		0	0.640	0.618	0.108
C28		0	1.279	1.225	0.327

Produced cements (MC1-MC2) were qualified, and their chemical and physical properties presented in [Tables 9](#) and [10](#) respectively.

**Table 9.** Chemical properties of MCs

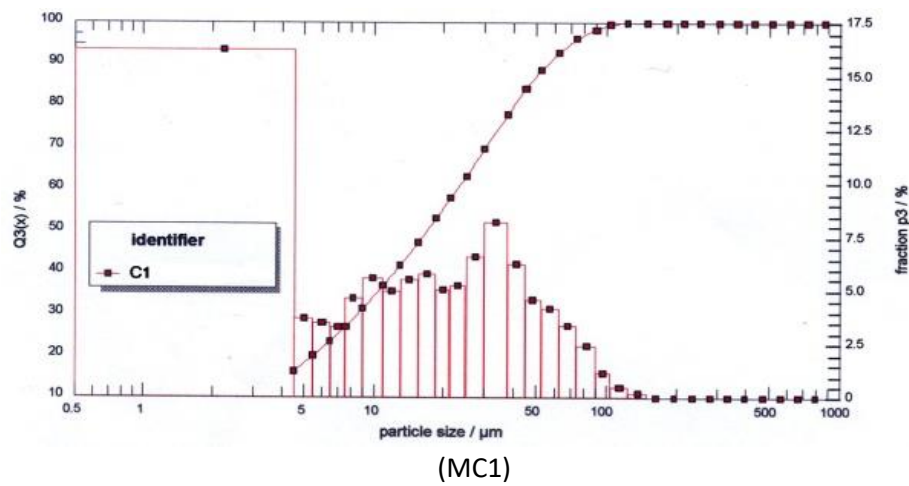
Compound/Property	MC1	MC2	MC3	MC4
Silica (SiO <sub>2</sub> )	22.26	21.17	22.03	23.86
Alumina (Al <sub>2</sub> O <sub>3</sub> )	3.86	4.82	5.30	4.77
Iron oxide (Fe <sub>2</sub> O <sub>3</sub> )	4.03	3.62	3.43	0.63
Magnesium oxide (MgO)	3.18	2.91	1.02	2.48
Calcium oxide (CaO)	61.57	63.10	63.65	63.39
Sulfur trioxide (SO <sub>3</sub> )	2.86	2.57	2.57	2.09
Free CaO	0.39	0.45	1.00	0.87
C <sub>3</sub> S	41.62	47.08	43.84	37.82
C <sub>2</sub> S	32.44	26.72	30.09	39.82
C <sub>3</sub> A	3.42	6.65	8.24	11.57
C <sub>4</sub> AF	12.25	10.77	10.45	1.92
Lime saturation factor (LSF)	88.58	91.71	90.71	87.02
Silica modulus	2.82	2.57	2.52	4.42
Alumina modulus	0.96	1.33	1.54	7.57

**Table 10.** Physical properties of MCs

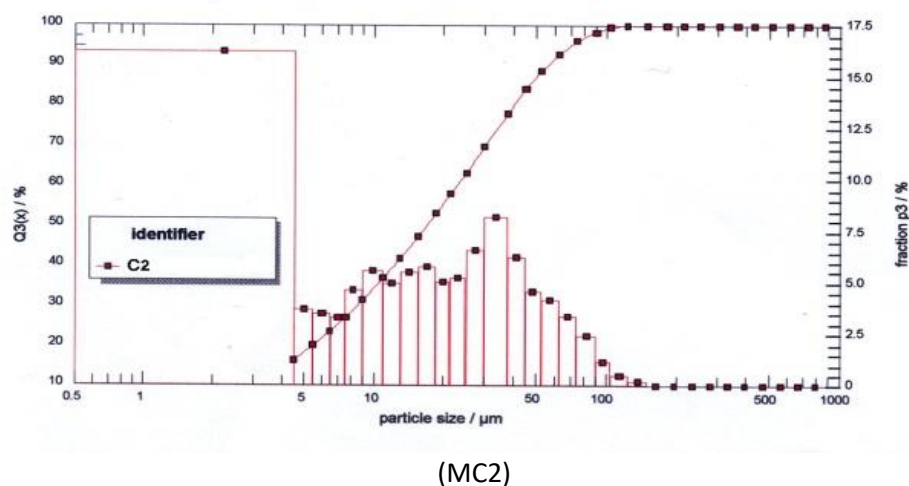
Property	MC1	MC2	MC3	MC4
Specific surface, cm <sup>2</sup> /gr	3100	3277	3464	3270
Initial setting time, min	235	225	210	265
Final setting time, min	292	288	265	310
Loss on ignition (LOI) at 975°C	1.22	1.34	1.20	2.01

Sieve analysis of produced types of cement determined using laser particle size analyzer method and the results

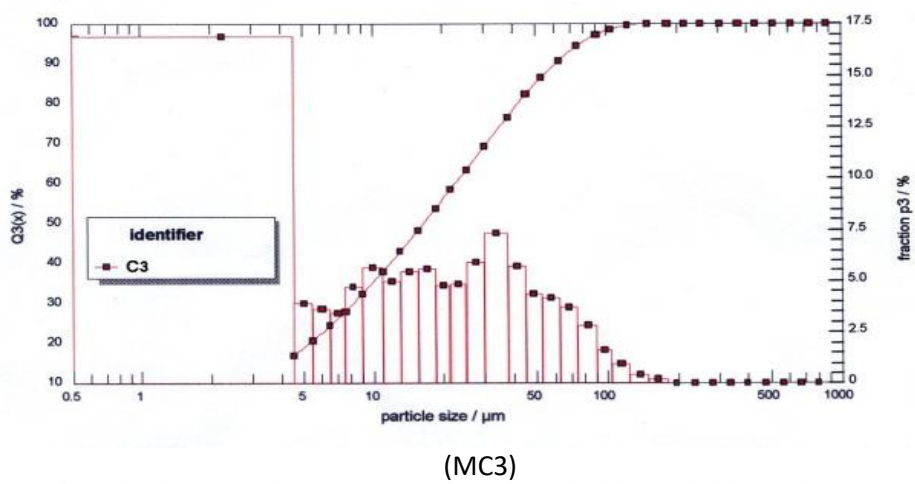
demonstrated in [Figure 8](#). As seen, acceptable particle size was found for all simulated cement.



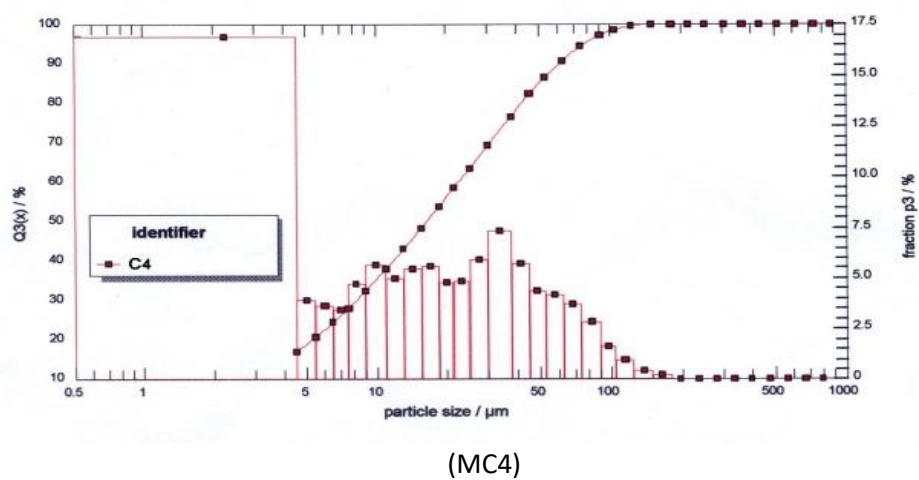
(MC1)



(MC2)



(MC3)



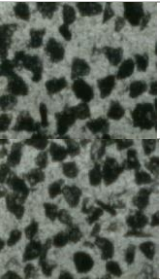
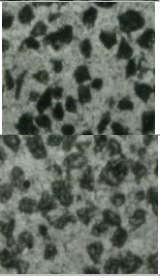
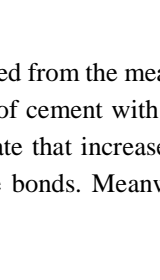

(MC4)

Figure 8. Particle size distribution of MCs

A microscopic study was conducted to determine the formed oxide phase of simulated cement. The summary of

this study is presented in [Table 11](#).

**Table 11.** Microscopic study of simulated cement

Type	Micrograph	Composition	Frequency, %	Size, $\mu\text{m}$		
				Max	Min	Distr.
MC1		Alite	44-48	20	10	13
		Belite	32-35	18	10	15
MC2		Alite	50-54	25	13	16
		Belite	23-25	20	10	15
MC3		Alite	60-63	20	10	15
		Belite	12-15	20	10	14
MC4		Alite	51-54	15	7	10
		Belite	23-25	20	5	12

The results obtained from the measurement of the chloride in samples made of cement with pure C<sub>3</sub>A (5, 8, 10, and 12 percent) indicate that increase in cement C<sub>3</sub>A content increases chloride bonds. Meanwhile, free chlorides and

chloride bonds decrease through an increase in C<sub>3</sub>A. [Figure 9](#) and [10](#) show the trend of increase in chloride bond through an increase in cement C<sub>3</sub>A content in samples made with NaCl and CaCl<sub>2</sub>, respectively.

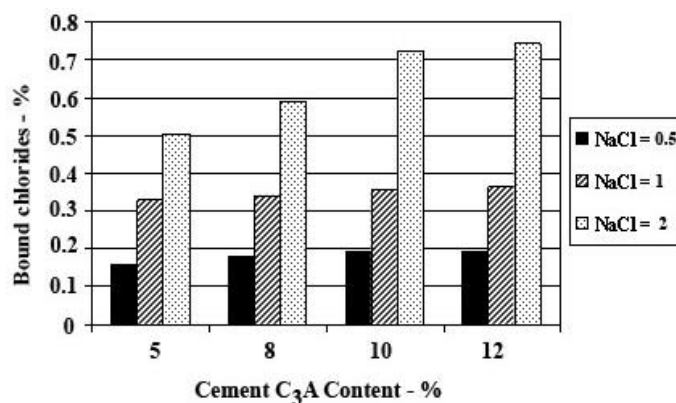


**Figure 9.** Trend of increase in bound chlorides through increase in cement C<sub>3</sub>A content (samples made of Pure C<sub>3</sub>A and NaCl)

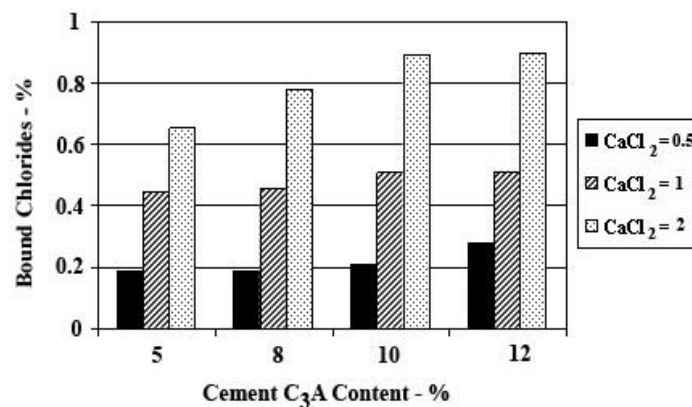


**Figure 10.** Trend of increase in bound chlorides through increase in cement C<sub>3</sub>A content (samples made of Pure C<sub>3</sub>A and CaCl<sub>2</sub>)

This paper studied the chloride binding of cement pastes with different C<sub>3</sub>A contents when exposed to CaCl<sub>2</sub> and

NaCl solutions. The chloride binding of the cement pastes exposed to CaCl<sub>2</sub>, and NaCl solutions can be divided into

three parts: 1) the formation of Friedel's salt; 2) the formation of calcium oxychloride; 3) adsorption of  $\text{Cl}^-$  ions by C-S-H. TGA was used to quantify the simulated  $\text{C}_3\text{A}$ . Standard test methods as per ASTM C1152 and ASTM C1218 were utilized to measure the acid-soluble and water-soluble chloride in prepared specimens, respectively. The addition of  $\text{C}_3\text{A}$  leads to a higher amount of Friedel's salt formed in the cement paste. The chemistry of the materials can be used to estimate the chloride binding associated with Friedel's salt. In the case of chloride ingress into the concrete or availability of chloride-contaminated concrete material (like in aggregates and cement), chloride ions could be found in

three states; free chlorides in pore solution, physically absorbed or bonded with hydrated components, and  $\text{C}_3\text{A}$ . As known, from the viewpoint of corrosion processes, the free chlorides have the governing effects. Chloride ions bind with  $\text{C}_3\text{A}$  and form Friedel's salt ( $\text{C}_3\text{A} \cdot \text{CaCl}_2 \cdot 10\text{H}_2\text{O}$ ). The chloride binding capacity of cement, is strongly determined by the  $\text{C}_3\text{A}$  of cement. Water-soluble chlorides have no contributions to chloride binding and are free in the pore solution. Acid-soluble ones included the water-soluble chlorides and were bound with the  $\text{C}_3\text{A}$  component of cement. Generally, the measurements of chlorides of concrete or paste include the water-soluble ions and are bound with  $\text{C}_3\text{A}$ .

## 4. CONCLUSION

Based on the obtained results, the following conclusions could be drawn: - The results showed that in cement samples made with different percentages of  $\text{C}_3\text{A}$  (5, 8, 10, and 12) with increasing the amount of  $\text{C}_3\text{A}$ , the chloride ions binding had been increased. - The amount of acid-soluble and water-soluble chloride for  $\text{NaCl}$  and  $\text{CaCl}_2$  cations decreased with an increase of the  $\text{C}_3\text{A}$ , indicating a better chloride ion binding potential. - For cations of  $\text{NaCl}$  and  $\text{CaCl}_2$ , at concentration levels, less

than about 1.3%, the changes in  $\text{C}_3\text{A}$  are ignorable in acid-soluble chloride. - For cations of  $\text{CaCl}_2$ , the increase of  $\text{C}_3\text{A}$  is distinguished in water-soluble chloride in comparison with  $\text{NaCl}$  cations. -  $\text{CaCl}_2$  cations have more chloride binding capacity than  $\text{NaCl}$  ones, so in areas contaminated with  $\text{NaCl}$  ions, it is recommendable to use the more  $\text{C}_3\text{A}$  content in the Portland cement.

### FUNDING/SUPPORT

Not mentioned any Funding/Support by authors.

### ACKNOWLEDGMENT

The authors appreciate the financial and scientific support of BHRC for experimental tests of this research.

### AUTHORS CONTRIBUTION

This work was carried out in collaboration among all authors.

### CONFLICT OF INTEREST

The author (s) declared no potential conflicts of interests with respect to the authorship and/or publication of this paper.

## 5. REFERENCES

- [1] Chen P, Ma B, Tan H, Liu X, Zhang T, Li C, Yang Q, Luo Z. Utilization of barium slag to improve chloride-binding ability of cement-based material. *Journal of Cleaner Production*. 2021 Feb 10;283:124612. [\[View at Google Scholar\]](#); [\[View at Publisher\]](#).
- [2] Yuan Q, Shi C, De Schutter G, Audenaert K, Deng D. Chloride binding of cement-based materials subjected to external chloride environment—a review. *Construction and building materials*. 2009 Jan 1;23(1):1-3. [\[View at Google Scholar\]](#); [\[View at Publisher\]](#).
- [3] Nielsen EP, Herfort D, Geiker MR. Binding of chloride and alkalis in Portland cement systems. *Cement and Concrete Research*. 2005 Jan 1;35(1):117-23. [\[View at Google Scholar\]](#); [\[View at Publisher\]](#).
- [4] Hirao H, Yamada K, Takahashi H, Zibara H. Chloride binding of cement estimated by binding isotherms of hydrates. *Journal of Advanced Concrete Technology*. 2005;3(1):77-84. [\[View at Google Scholar\]](#); [\[View at Publisher\]](#).
- [5] Ipavec A, Vuk T, Gabrovšek R, Kaučič V. Chloride binding into hydrated blended cements: The influence of limestone and alkalinity. *Cement and Concrete Research*. 2013 Jun 1;48:74-85. [\[View at Google Scholar\]](#); [\[View at Publisher\]](#).
- [6] Enevoldsen JN, Hansson CM, Hope BB. Binding of chloride in mortar containing admixed or penetrated chlorides. *Cement and Concrete Research*. 1994 Jan 1;24(8):1525-33. [\[View at Google Scholar\]](#); [\[View at Publisher\]](#).
- [7] Al-Hussaini MJ, Sangha CM, Plunkett BA, Walden PJ. The effect of chloride ion source on the free chloride ion percentages in OPC mortars. *Cement and concrete research*. 1990 Sep 1;20(5):739-45. [\[View at Google Scholar\]](#); [\[View at Publisher\]](#).

[8] Arya C, Buenfeld NR, Newman JB. Factors influencing chloride-binding in concrete. *Cement and Concrete research*. 1990 Mar 1;20(2):291-300. [\[View at Google Scholar\]](#); [\[View at Publisher\]](#).

[9] Hansson CM, Frølund T, Markussen JB. The effect of chloride cation type on the corrosion of steel in concrete by chloride salts. *Cement and Concrete Research*. 1985 Jan 1;15(1):65-73. [\[View at Google Scholar\]](#); [\[View at Publisher\]](#).

[10] Shi C, Hu X, Wang X, Wu Z, Schutter GD. Effects of chloride ion binding on microstructure of cement pastes. *Journal of Materials in Civil Engineering*. 2017 Jan 1;29(1):04016183. [\[View at Google Scholar\]](#); [\[View at Publisher\]](#).

[11] Liu J, Ou G, Qiu Q, Chen X, Hong J, Xing F. Chloride transport and microstructure of concrete with/without fly ash under atmospheric chloride condition. *Construction and Building Materials*. 2017 Aug 15;146:493-501. [\[View at Google Scholar\]](#); [\[View at Publisher\]](#).

[12] Yi C, Ma H, Zhu H, Li W, Xin M, Liu Y, Guo Y. Study on chloride binding capability of coal gangue based cementitious materials. *Construction and Building Materials*. 2018 Apr 10;167:649-56. [\[View at Google Scholar\]](#); [\[View at Publisher\]](#).

[13] Qiao C, Suraneni P, Ying TN, Choudhary A, Weiss J. Chloride binding of cement pastes with fly ash exposed to CaCl<sub>2</sub> solutions at 5 and 23° C. *Cement and Concrete Composites*. 2019 Mar 1;97:43-53. [\[View at Google Scholar\]](#); [\[View at Publisher\]](#).

[14] Xu J, Zhang C, Jiang L, Tang L, Gao G, Xu Y. Releases of bound chlorides from chloride-admixed plain and blended cement pastes subjected to sulfate attacks. *Construction and Building Materials*. 2013 Aug 1;45:53-9. [\[View at Google Scholar\]](#); [\[View at Publisher\]](#).

[15] Bahman-Zadeh F, Ramezani-pour AA, Zolfagharnasab A. Effect of carbonation on chloride binding capacity of limestone calcined clay cement (LC3) and binary pastes. *Journal of Building Engineering*. 2022 Jul 15;52:104447. [\[View at Google Scholar\]](#); [\[View at Publisher\]](#).

[16] Sun M, Sun C, Zhang P, Liu N, Li Y, Duan J, Hou B. Influence of carbonation on chloride binding of mortars made with simulated marine sand. *Construction and Building Materials*. 2021 Oct 11;303:124455. [\[View at Google Scholar\]](#); [\[View at Publisher\]](#).

[17] Wang GM, Kong Y, Shui ZH, Li Q, Han JL. Experimental investigation on chloride diffusion and binding in concrete containing metakaolin. *Corrosion engineering, science and technology*. 2014 Jun 1;49(4):282-6. [\[View at Google Scholar\]](#); [\[View at Publisher\]](#).

[18] Cheewaket T, Jaturapitakkul C, Chalee W. Long term performance of chloride binding capacity in fly ash concrete in a marine environment. *Construction and Building Materials*. 2010 Aug 1;24(8):1352-7. [\[View at Google Scholar\]](#); [\[View at Publisher\]](#).

[19] Zunino F, Scrivener K. Factors influencing the sulfate balance in pure phase C3S/C3A systems. *Cement and Concrete Research*. 2020 Jul 1;133:106085. [\[View at Google Scholar\]](#); [\[View at Publisher\]](#).

[20] ASTM C1218-99 Standard Test Method for Water-Soluble Chloride in Mortar and Concrete, ASTM International, West Conshohocken, PA, USA. [\[View at Publisher\]](#).

[21] ASTM C1152-04 Standard Test Method for Acid-Soluble Chloride in Mortar and Concrete, ASTM International, West Conshohocken, PA, USA. [\[View at Publisher\]](#).